This article was downloaded by:
On: *25 January 2011*
Access details: *Access Details: Free Access*
Publisher *Taylor & Francis*
Informa Ltd Registered in England and Wales Registered Number: 1072954 Registered office: Mortimer House, 37-41 Mortimer Street, London W1T 3JH, UK

Separation Science and Technology
Publication details, including instructions for authors and subscription information:
http://www.informaworld.com/smpp/title~content=t713708471

Flow Field-Flow Fractionation of Polyacrylamides: Commercial Flocculants

R. Hecker[a]; P. D. Fawell[b]; A. Jefferson[c]; J. B. Farrow[b]
[a] Max-Planck-Institut für Kolloid-und Grenzflächenforschung, Germany [b] CSIRO MINERALS, BENTLEY, WESTERN AUSTRALIA, AUSTRALIA [c] SCHOOL OF APPLIED CHEMISTRY, CURTIN UNIVERSITY OF TECHNOLOGY, WESTERN AUSTRALIA, AUSTRALIA

Online publication date: 20 March 2000

To cite this Article Hecker, R. , Fawell, P. D. , Jefferson, A. and Farrow, J. B.(2000) 'Flow Field-Flow Fractionation of Polyacrylamides: Commercial Flocculants', Separation Science and Technology, 35: 4, 593 — 612
To link to this Article: DOI: 10.1081/SS-100100178
URL: http://dx.doi.org/10.1081/SS-100100178

PLEASE SCROLL DOWN FOR ARTICLE

Full terms and conditions of use: http://www.informaworld.com/terms-and-conditions-of-access.pdf

This article may be used for research, teaching and private study purposes. Any substantial or systematic reproduction, re-distribution, re-selling, loan or sub-licensing, systematic supply or distribution in any form to anyone is expressly forbidden.

The publisher does not give any warranty express or implied or make any representation that the contents will be complete or accurate or up to date. The accuracy of any instructions, formulae and drug doses should be independently verified with primary sources. The publisher shall not be liable for any loss, actions, claims, proceedings, demand or costs or damages whatsoever or howsoever caused arising directly or indirectly in connection with or arising out of the use of this material.

SEPARATION SCIENCE AND TECHNOLOGY, **35**(4), pp. 593–612, 2000

Flow Field-Flow Fractionation of Polyacrylamides: Commercial Flocculants

R. HECKER*
SCHOOL OF APPLIED CHEMISTRY
CURTIN UNIVERSITY OF TECHNOLOGY
GPO BOX U1987, WESTERN AUSTRALIA 6845, AUSTRALIA

P. D. FAWELL†
CSIRO MINERALS
PO BOX 90, BENTLEY, WESTERN AUSTRALIA 6102, AUSTRALIA

A. JEFFERSON
SCHOOL OF APPLIED CHEMISTRY
CURTIN UNIVERSITY OF TECHNOLOGY
GPO BOX U1987, WESTERN AUSTRALIA 6845, AUSTRALIA

J. B. FARROW
CSIRO MINERALS
PO BOX 90, BENTLEY, WESTERN AUSTRALIA 6102, AUSTRALIA

Downloaded At: 11:01 25 January 2011

ABSTRACT

The coupling of flow field-flow fractionation (flow FFF) and a multiangle laser light-scattering (MALLS) detector enables absolute measurements of weight-averaged molecular mass distributions for polymer solutions. The technique, applied recently to polyacrylamide (PAAm) standards, has been extended to commercial nonionic flocculants in an aqueous environment. A mass distribution is achieved in less than 2 hours per sample, which offers a significant improvement over size-exclusion chromatography in terms of throughput. While the fractionation of commercial PAAm solutions generally follows the same pattern as for lower molecular mass stan-

* Present address: Kolloidchemie Gruppe, Max-Planck-Institut für Kolloid-und Grenzflächenforschung, Am Mühlenberg, D-14476 Golm, Germany.
† To whom correspondence should be addressed.

Copyright © 2000 by Marcel Dekker, Inc. www.dekker.com

ORDER REPRINTS

dards, there is also strong evidence of polymer agglomeration. In some samples these agglomerates are of sufficient size to interfere with the fractionation due to the parallel separation mechanisms of the FFF. The extent of agglomerate formation was dependent upon solution age and may be a factor in age-related loss of flocculant activity. Significant dispersion of such species was achieved by dilution of polymer in salt solutions prior to injection into the FFF cell.

Key Words. Flow field-flow fractionation; Multiangle laser light scattering; Polyacrylamide; Flocculants; Molecular mass distribution; Agglomerates

INTRODUCTION

The effects of mixing, shear, and particulate surface chemistry on flocculation have been extensively studied (1–3). A missing component for flocculation research is a method to reliably measure the molecular mass distribution of the flocculant. Size-exclusion chromatography is a common tool for characterization of polymer mass distributions, but the viscosity and shear-sensitivity of high molecular mass polyacrylamide (PAAm) is incompatible with a packed column technique. In a previous publication (4) it was shown that the flow field-flow fractionation–multiangle laser light scattering (flow FFF–MALLS) technique provides an absolute measure of the molecular mass distribution of polyacrylamide standards. This work reports an extension of flow FFF–MALLS to characterize commercial, ultrahigh molecular mass polyacrylamides used as flocculants in mineral processing and other industries.

The field-flow fractionation (FFF) family of techniques features an open channel design of small surface area (<0.01 m^2) such that analytical error from adsorptive loss and shearing are limited (5). For samples of less than 1 μm diameter, FFF relies on competition between the field and backdiffusion off the accumulation wall. The narrow ribbon channel is sufficiently thin to cause the carrier flow to occupy a parabolic flow profile and smaller, more diffusive samples occupy a mean faster-moving lamina. Subtechniques of FFF arise from the nature of the applied field, and both thermal gradient (thermal FFF) and crossflow (flow FFF) have been shown to be effective for the analysis of synthetic polymers (6–8). The universal nature of flow FFF, in that all samples are influenced by crossflow, is advantageous, but the presence of a membrane within the channel may lead to excess band broadening due to surface roughness and interactions between the solute and the membrane. Thermal FFF was found ineffective in aqueous media due to poor thermal diffusion (9–11).

The use of light scattering to determine the macromolecular parameters of root-mean-square radii and molecular mass batchwise has been described elsewhere (12). Using this instrument in a flow arrangement, in conjunction

Downloaded At: 11:01 25 January 2011

Copyright © Marcel Dekker, Inc. All rights reserved.

MARCEL DEKKER, INC.
270 Madison Avenue, New York, New York 10016

ORDER REPRINTS

with a concentration-sensitive device, allows light scattering to be used for chromatographic detection (13).

THEORY

Flow Field-Flow Fractionation

FFF possesses a reliable theoretical basis for the prediction of elution times, presented in full elsewhere (14–16). For submicron particles the "normal" mode of separation (Fig. 1a) dominates under most conditions, and flow FFF retention times depend solely upon sample diffusion coefficients.

For polydisperse samples the problem of producing separation within a reasonable experimental time arises. For FFF this may be solved by allowing the field strength to decay over the course of the separation. Under such conditions the diffusion coefficient D is related to the retention time t_r by

$$D = \frac{w^2}{6}\frac{\dot{V}_c^i}{\dot{V}}\left[\tau\left(\exp\left(\frac{t_r}{\tau}\right) - 1\right)\right]^{-1} \quad (1)$$

where w is the thickness of the FFF channel, with axial channel flow $\dot{V}$, and the crossflow decays exponentially from an initial $\dot{V}_c^i$ at a time constant τ immediately after the sample loading and stopflow period (4). These expressions are for model conditions where extraneous sample—membrane interactions do not occur.

A parallel mechanism for the separation of samples by the FFF technique arises where the center of mass of the particle is affected by the channel flow stream, as shown schematically in Fig. 1(b). Separation occurs on the basis of diameter rather than diffusion and is significant mainly for particles of greater than 1 μm diameter. This "steric mode" has been employed for the high-speed separation of supramicron particles (17). The elution in the steric mode is in

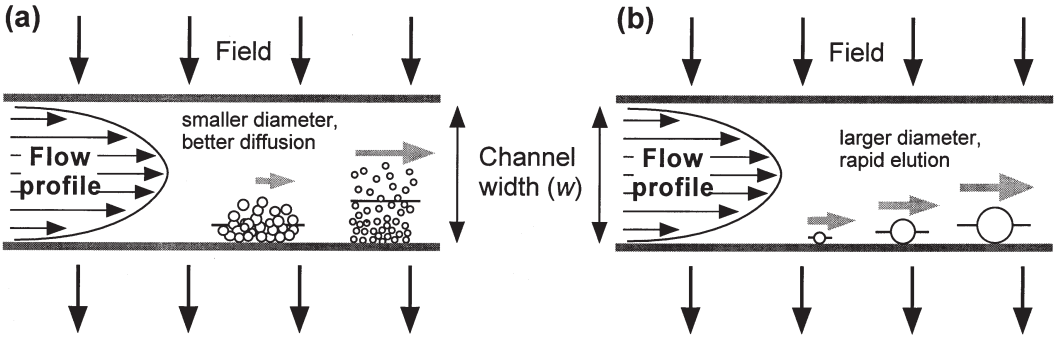

FIG. 1 Mechanisms of FFF separation for (a) submicron-sized solutes by the "normal" mode and (b) supramicron solutes by the "steric" mode.

Downloaded At: 11:01 25 January 2011

Copyright © Marcel Dekker, Inc. All rights reserved.

MARCEL DEKKER, INC.
270 Madison Avenue, New York, New York 10016

ORDER REPRINTS

the order largest to smallest diameter (the reverse of the progression under normal mode). For a particle of diameter d, the retention time, expressed as a ratio to the void time t^0, is given according to

$$\frac{t_r}{t^0} = \frac{w}{3\gamma d} \tag{2}$$

The parameter γ is an empirical figure of order unity, introduced to account for lift forces acting upon the particle. The reversed elution leads to coelution for polydisperse samples, where the largest diameter samples affected by the steric mode elute simultaneously with the very smallest progressing by the normal mode. The critical size where mechanism inversion occurs is not well defined and is dependant upon fractionation conditions (18), shifting to as low as 0.23 μm for very high flow rates in a thin channel (19). In contrast to the normal mode, fractionation by the steric mode is harder to predict due to the complication of lift forces. The theory does not as yet allow for calculation of size on the basis of elution time from first principles. Published studies using the steric mode for separation have been on "hard" spheres, such as polymer latex standards or inorganic particles, and the effect of such elution on "soft," flexible bodies is unknown.

Light Scattering

Extensive theory for the MALLS laser photometer is provided in Wyatt (12), summarized in Hecker et al. (4). Coupling a fractionator with an on-line concentration detector allows calculation of the weight-averaged molecular mass from the angular dependence of the light scattering according to the following equation (shown here only to second order):

$$\frac{R_\theta}{K^* c} = M_w P(\theta) - 2A_2 M_w^2 P^2(\theta) c + \cdots \tag{3}$$

where R_θ is the scattering intensity excess to solvent scattering for solute of concentration c and weight-averaged molecular mass M_w at subtended angle θ, while the K^* term is an optical constant and A_2 is the second virial coefficient. The function $P(\theta)$ is an architecture function dependant upon the proximity of scattering centers throughout the molecule, which for a random-coil conformation is

$$P(\theta) = 1 - \frac{2\mu^2 \langle r^2 \rangle}{3!} + \cdots \tag{4}$$

where $\mu = (4\pi/\lambda_0) \sin(\theta/2)$ and λ_0 is the vacuum wavelength of the incident light. The value of $\langle r^2 \rangle^{0.5}$ is known as the root-mean-square radius ("rms radius"), derived from the distribution of the scattering centers.

Downloaded At: 11:01 25 January 2011

Copyright © Marcel Dekker, Inc. All rights reserved.

MARCEL DEKKER, INC.
270 Madison Avenue, New York, New York 10016

ORDER REPRINTS

From these light-scattering equations it is can been seen that plotting R_θ/K^*c from the detector set versus $\sin^2(\theta/2)$ gives, upon extrapolation to $\theta = 0°$, the value for M_w, provided that the concentration for the eluent slice is known accurately. The angular dependence of the scattering is a function of $\langle r^2 \rangle^{0.5}$, therefore both the molecular mass and rms radius can be obtained from a single light-scattering experiment.

Molecular Mass Calculation

Molecular mass can be calculated in two ways with a MALLS detector characterizing FFF eluant. Direct measurements arise when the FFF acts passively, separating the sample into near monodisperse slices for treatment by the MALLS detector according to the requirements of Eq. (3). Molecular masses may also be calculated indirectly from FFF retention times. Equation (1) shows retention is dependent solely upon the diffusion coefficient, and therefore the molecular mass, for flow FFF under normal mode operations. The indirect method relies upon ideal circumstances where the polymer coils do not interact with the membrane (retarding their passage through the cell) or alter configuration (thereby changing their hydrodynamic diameter and diffusion coefficient).

In a previous publication (4) it was demonstrated that the direct (light-scattering) method was preferred for the determination of the molecular mass distribution of PAAm standards. The molecular masses presented here were derived from the direct method by using the data processing parameters given in the Experimental section.

EXPERIMENTAL

Reagents

Purified water was delivered from a Milli-Q 185 unit with resistivity > 18 $M\Omega \cdot cm^{-1}$ (Millipore, Bedford, MA, USA). The carrier solution for the fractionation used AR grade nitric acid (BDH, Poole, England) in Milli-Q water adjusted to pH 3.8 ± 0.1, vacuum filtered to 0.22 μm (Millipore, type GV).

The commercial PAAm materials were obtained from two different manufacturers, designated companies **A** and **B**. In this study, for reasons of commercial sensitivity, these products are described only by the codes given in Table 1. All are used as flocculants in the mineral processing industries except **B3,** which is used for slurry rheology modification. Milli-Q water for the polymer solutions was freshly filtered through a 0.1-μm filter (Millipak 40 "gamma gold," Millipore). PAAm stock solutions were produced at approximate industrial concentrations by adding portions of polymer piecewise to water pretared in a screwtop glass jar, then shaken overnight on an orbital shaker

Downloaded At: 11:01 25 January 2011

Copyright © Marcel Dekker, Inc. All rights reserved.

MARCEL DEKKER, INC.
270 Madison Avenue, New York, New York 10016

ORDER REPRINTS

TABLE 1
Commercial Polyacrylamides Used in This Study, with their Mean Molecular Masses (cited by manufacturer and light scattering), and Viscosity (reported as extrapolation to infinite dilution). The Stock Concentrations Are Those Used for Fractionation

PAAm designation	Stock concentration ($mg \cdot mL^{-1}$)	Mean molecular mass		Capillary viscosity[b] ($mL \cdot mg^{-1}$)
		Cited	MALLS[a] M_w	
Company **A**:				
A1	3.98	$1.9–2.2 \times 10^7$	2.02×10^7	2.21 (R^2 0.98)
A2	4.08	$1.5–1.7 \times 10^7$	1.08×10^7	0.73 (R^2 0.95)
Company **B**:				
B1	3.85	$2.2–2.5 \times 10^7$	2.32×10^7	0.75 (R^2 0.98)
B2	4.59	$1.6–1.9 \times 10^7$	1.30×10^7	1.47 (R^2 0.97)
B3	4.12	$7–9 \times 10^6$	1.16×10^7	0.41 (R^2 0.95)

[a] Solutions unfiltered, 5th order Debye fit, dn/dc 0.190 $mg \cdot mL^{-1}$, in 0.1 NaCl.
[b] Ubbelohde viscometer (No. 75, 0.01017 $cSt\text{-}s^{-1}$) at 35.0°C.

Downloaded At: 11:01 25 January 2011

at 150 ± 5 rpm (Braun TM-1, Basel, Switzerland). All solutions were prepared in a laminar flow cabinet (Gelman HWS, Ann Arbor, MA) to minimize particulate contamination. The stock concentrations used for each product are listed in Table 1. For the low-concentration injections of **A1,** solutions of 2.07 and 0.50 $mg \cdot mL^{-1}$ were also prepared.

During the aging experiments the aqueous polymer solutions sat on a benchtop out of direct sunlight and free of any mechanical agitation. Other factors, such as temperature (23 ± 2°C) and illumination, were ambient laboratory conditions prevailing at the time of the experiment.

Chemical Analysis of the Polymer

The chemical properties of the PAAm samples were determined by both quantitative ^{13}C NMR (20) and microanalysis. A concentrated sample of PAAm (3% w/v) was degraded ultrasonically by a XL2020 horn from Heat Systems (Farmingdale, NY, USA). Metal fines from the horn were removed by centrifugation (Hettich Mikro 12-24, Tuttlingen, Germany), and clarified polymer was loaded into the sample tube with a quantity of D_2O and *p*-dioxana (standard, δ67.4). Carbon specta were recorded on a 200-MHz machine (Varian Gemini, Palo Alto, CA, USA) using an inverse gate decoupling to suppress the nuclear Overhauser effect requiring a 12.0-μs pulse and 7.0 s relaxation time and needing 10^4 transients for sufficient signal strength. Quantization was made based on the δ184 acrylate versus δ180 amide carbonyl signals, while imides could be detected at δ175. No PAAm samples showed detectable hydrolysis or exhibited imidization.

Copyright © Marcel Dekker, Inc. All rights reserved.

ORDER REPRINTS

Apparatus

The apparatus was described in the previous publication of this research (4), and only salient details are repeated here.

The flow FFF cell used was a model F0-1000 from FFFractionation (Salt Lake City, UT, USA) with the accumulation wall covered by a membrane of regenerated cellulose (nominal MWCO 10^4) from FFFractionation. The channel shape was defined by a Teflon spacer (0.25 mm thick, 300 mm long, and 20 mm maximum width), and the final 20 mm of the channel immediately prior to the sample outlet was fitted with a frit outlet device. Channel and crossflow was delivered by dual-piston pumps (LC10-AD, Shimadzu, Kyoto, Japan), and the crossflow was continually recycled. The channel flow was subject to a 10-μm sink filter, an in-line degasser unit (Shimadzu GT-102), and 0.1-μm final filtration (Millipore type VV) before the sample injector (Rheodyne 7125, Cotati, CA, USA) and the FFF cell. The outlet flow splitting was controlled by a needle valve (Nupro, Willoughby, OH, USA) on the frit outlet line.

The introduction of the polymer solution into the sample loop required slow loading, with a typical 100 μL load taking 1.5 minutes. In all cases the syringe was rinsed with five loadings of carrier liquid, as was the injector.

Detectors for the FFF effluent were multiangle laser light scattering (Dawn-DSP from Wyatt Technology, Santa Barbara, CA, USA) and differential refractometer ("DRI") Optilab 903 (Wyatt Technology). The light-scattering detector used a 632-nm vertically polarized laser. The refractometer used a 632-nm source and a 10-mm P100 cell maintained at 35.0 ± 0.1°C by a waterbath to eliminate thermal drift. The refractometer was reset before each fractionation experiment. Data accumulation for the detectors used Wyatt Technology ASTRA 4.20 software.

Standard PAAm analysis flow rates were a channel flow of 0.3 $mL \cdot min^{-1}$ and an initial field flow of 0.4 $mL \cdot min^{-1}$. A channel outlet flow split ratio (waste:detectors) of 2:1 was used. The sample load protocol involved a 5.5-minute period to accumulate baseline detector signals, a 0.5-minute load time to load the sample from the injector loop to the fractionator cell, and finally a 4.0-minute stopflow time before fractionation commenced. The field decay commenced immediately after the stopflow period with a time constant of 60 minutes. Therefore, the first 10.0 minutes of all elution profiles shown represent sample loading and stopflow.

Light-Scattering Data Processing

Concentration measurements, required for molecular mass determinations, were obtained with the DRI detector. A refractive index increment (dn/dc) of 0.190 $mL \cdot g^{-1}$ was measured for PAAm in the carrier liquid at 35°C. For the chromatographic output, fitting by the Debye formalism with a fourth-order

Downloaded At: 11:01 25 January 2011

Copyright © Marcel Dekker, Inc. All rights reserved.

MARCEL DEKKER, INC.
270 Madison Avenue, New York, New York 10016

ORDER REPRINTS

angular dependence gave the most reasonable results with the lowest error. This was used for all experiments.

Viscosity

An Ubbelohde capillary viscometer (No. 75, 0.01017 $cSt \cdot s^{-1}$) was used to measure dilute polymer solution viscosities at 35.0 ± 0.1°C. Measurements were made over a range of concentrations and extrapolated to infinite dilution.

Static Light-Scattering

The MALLS detector was also used for batch determinations of molecular mass, using described calibration and normalization methods. Stock polymer solution was diluted 1:1 with 0.22 μm filtered 0.20 M NaCl. Solutions were extruded slowly from 10 mL syringes from a syringe pump at 8 $mL \cdot h^{-1}$ into a length of 0.51 mm I.D. PEEK tubing. Solvent offsets were taken from 0.10 M NaCl. Processing of the light-scattering data used DAWN 3.01 and AURORA softwares from Wyatt Technology.

RESULTS AND DISCUSSION

Viscometry and Mean Molecular Mass

Solution viscosities are the most commonly used approach for the characterization of flocculants, mainly because the technique is simple and inexpensive. However, the derivation of molecular masses from viscosities requires numerous assumptions and, in the absence of high molecular mass standards, invariably introduces significant errors from extrapolation. The absolute measurements of molecular mass by static light scattering (MALLS) offers greater accuracy although it only provides an average solution value. Table 1 compares nominal and measured molecular masses, together with relative solution viscosities. While the mean M_w follows a similar trend to the nominal molecular masses, no such trend can be seen from the solution viscosities. This may reflect different levels of polymer agglomeration in the solution (21). Clearly, some indication of the molecular mass distribution is required for proper characterization of these materials.

Commercial Flocculants versus Polyacrylamide Standards

Ideally, flow FFF fractionates PAAm on the basis of diffusion, indifferent to the source, to produce a near-monodisperse slice for subsequent characterization. In a recent publication (4) we showed such a self-consistency for PAAm standards. This consistency is reconfirmed by Fig. 2, where the elution time–molecular mass relationship of the standards is compared with the elu-

Downloaded At: 11:01 25 January 2011

Copyright © Marcel Dekker, Inc. All rights reserved.

MARCEL DEKKER, INC.
270 Madison Avenue, New York, New York 10016

ORDER REPRINTS

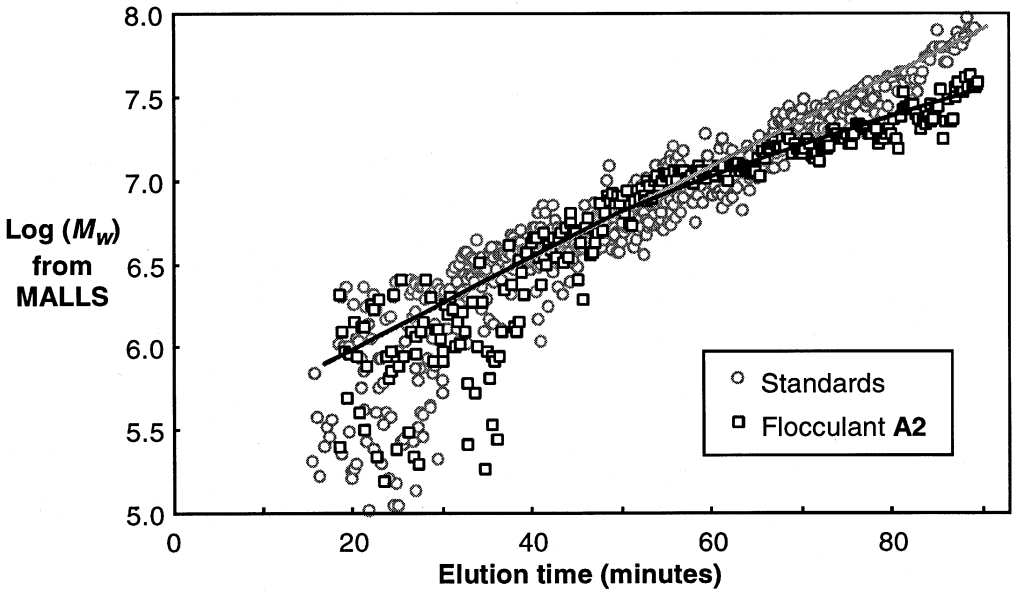

FIG. 2 Comparison of the fractionation of standards and commercial flocculant **A2.**

tion of the flocculant **A2.** The remarkable colinearity over most of the range shows again that elution is independent of source. However, at high retention (larger hydrodynamic radius) the measured molecular mass for flocculant **A2** levels off, deviating from the relationship seen for the PAAm standards.

Fractionation of Commercial Flocculants

The elution profile of the PAAm products from companies **A** and **B** are shown in Fig. 3(a) and 3(b), respectively. These clearly indicate differences in the molecular mass distributions. Table 1 states that the mean molecular mass of **A1** is much greater than that of **A2**. However, initial examination of Fig. 3(a) does not support this at all, with the broad distribution of **A2** displaying a greater fraction eluting at long retention times. **A1** gave a distinctly bimodal distribution, with a high concentration of rapidly eluting material. Agglomerates as large as 20 μm were found in a previous study of **A1** solutions (21). Agglomerates of this size would be expected to coelute with finer material according to the parallel normal/steric mode mechanisms of FFF, which could therefore explain these early peaks in the elution profile. For comparison, injection of 9.1 μm polystyrene latex eluted with a peak 7.2 minutes after the end of stopflow (raw elution time 17.2 minutes) under the fractionation conditions. This suggests the early peaks for **A1** may be agglomerate derived.

Additional evidence that the early peak of the **A1** elution profile is due to supramicron agglomerates is provided by Fig. 4, which compares light-scattering data for **A1** and **A2** at selected elution volume slices. The light-scatter-

Downloaded At: 11:01 25 January 2011

Copyright © Marcel Dekker, Inc. All rights reserved.

MARCEL DEKKER, INC.
270 Madison Avenue, New York, New York 10016

ORDER REPRINTS

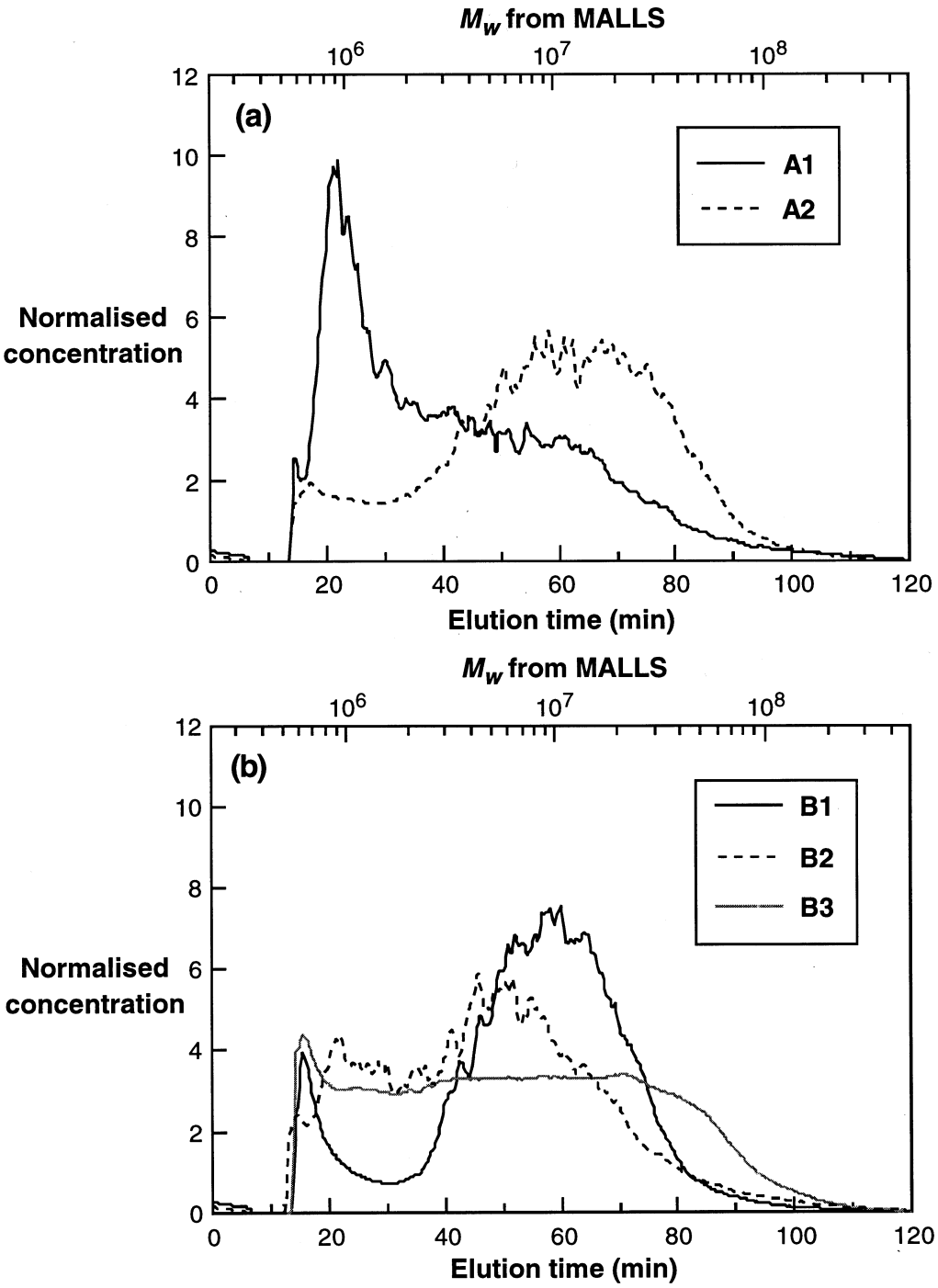

FIG. 3 Fractionation of commercial PAAm aged for 2 days under standard conditions. The M_w axis arises from the relation presented in Ref. 4 and is applicable only to discrete coils, not agglomerates. The refractometer (DRI) responses are normalized to stock PAAm injections.

Downloaded At: 11:01 25 January 2011

Copyright © Marcel Dekker, Inc. All rights reserved.

MARCEL DEKKER, INC.
270 Madison Avenue, New York, New York 10016

ORDER REPRINTS

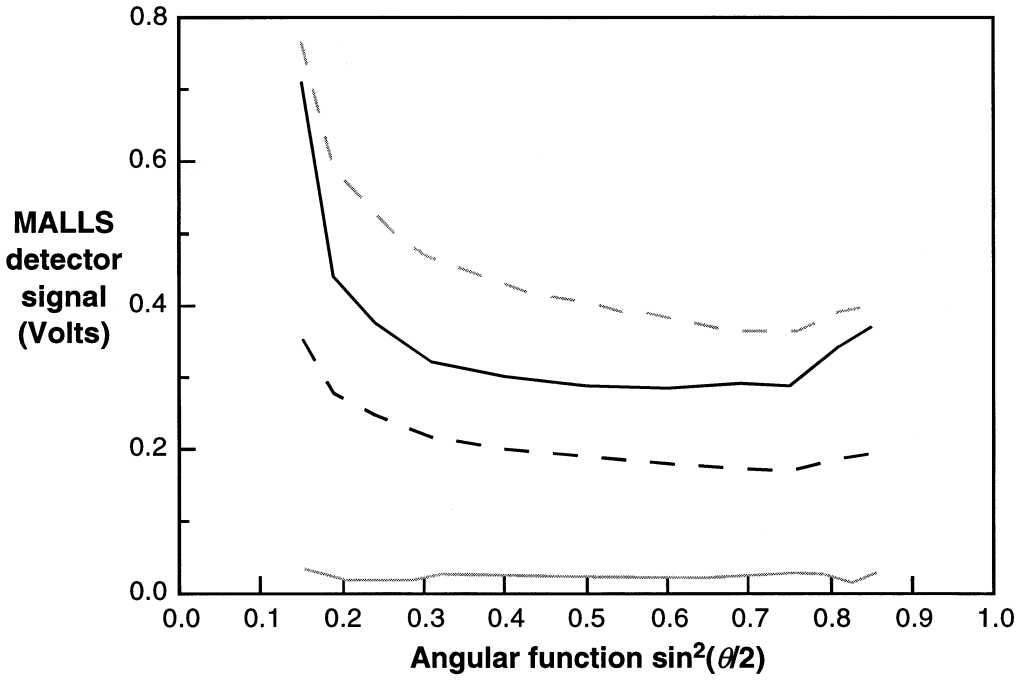

FIG. 4 Excess scattering of elution profiles from MALLS for a given elution time for **A1** (dark) and **A2** (light) at times 20 minutes (solid) and 60 minutes (dashed).

ing detector, in accordance with Eq. (3), has a scattering angular dependence determined by $P(\theta)$ which is a function of the rms radius of the polymer coil; specifically, a greater curvature identifies the presence of larger species. Comparing the angular dependence of the light scattering after 20 minutes elution, the **A2** curve is flat, indicating that materials eluting at this time behave as isotropic scattering bodies, and therefore must be sufficiently small to be subject to the normal elution mode. A slice at 60 minutes elution has a similar curvature for both **A2** and **A1** samples although the concentration differs, indicating that the material eluting at this time is the same size regardless of source as demonstrated by Fig. 2. The curvature of the **A1** sample after 20 minutes is greater than that at 60 minutes and identifies the presence of a larger species. Although light scattering is a function of both scatterer radius and concentration, the curvature proves that the early peak in the **A1** elution profile is due to agglomerates. To elute so early, the species must be of sufficient size to be subject to the FFF steric mechanism.

However, quantifying the size of the agglomerates of the **A1** elution is not simple, as sizing by the light scattering signal is influenced by the coeluting material. The superposition of the large, low concentration material (influencing predominantly the lower angle detectors) with the smaller, higher concentration (affecting all detectors more evenly) will provide a net angular dependence less than expected for the agglomerates alone. While the FFF theory

Downloaded At: 11:01 25 January 2011

Copyright © Marcel Dekker, Inc. All rights reserved.

MARCEL DEKKER, INC.
270 Madison Avenue, New York, New York 10016

ORDER REPRINTS

demonstrates retention based solely upon diffusion for submicron species, the complication of lift forces for agglomerates affected by the steric mechanism has so far meant there is no first-principles function for calculation of size from elution time.

The features of company **B** materials may be discussed within the context of those from company **A**. **B1** has the highest mean molecular mass and the lowest fraction of low molecular mass materials, with almost no agglomeration detected by MALLS. Sample **B2** has a much lower mean molecular mass but a capillary viscosity second only to **A1**, while the fractionation of **B2** indicates the presence of supramicron agglomerates in the fashion of **A1**. The low mean molecular mass samples **A2** and **B3** share a similarly wide elution profile, and a reason for this will be discussed later.

Aging Effects

The fractionation of stock **A2** with detection from the concentration-sensitive refractometer is shown by Fig. 5(a). From the elution profile the peak concentration of polymer elutes at 60 minutes which, using the relationship shown in Fig. 2, corresponds to a molecular mass of 12.5×10^6. A substantial amount elutes later than this peak, and the data reprocessed as a cumulative concentration profile are summarized in Table 2.

By concentration, about 25% of the polymer elutes as species with a mean molecular mass over 20×10^6. There is only a slight aging effect for **A2**; after 38 days there is no discernible difference to the mass distribution from the 15-day-old solution.

Hecker et al. (21) showed that agglomerates present in PAAm were dynamic and therefore solution aging is of concern. The elution profile of **A1** also reflects a clear aging effect (Fig. 5b). The supramicron peaks around 20 minutes shift to a later elution, which under a steric mechanism indicates a general decrease in size, and therefore agglomerate dispersion. Simultaneously, the free polymer coil peaks eluting later than 60 minutes (corresponding to the $15–25 \times 10^6$ PAAm) become increasingly dominant. These coils are subject to the normal mode mechanism. The effect may be attributed to (a) the agglomeration/entanglement of the smaller coils, (b) an increasing coil radius due to some swelling mechanism, (c) polymer conformation change, or (d) the erosion of agglomerates. The agglomeration of small coils is unlikely as it is not observed in the aging behavior of the otherwise identical **A2** sample. Significant swelling of the polymer is rejected as the polymer is already extensively solvated in solution. Conformation change is known to occur in PAAm solutions with aging (22), but a shift in elution of the magnitude that was observed is far too great. Therefore (d), the erosion of supramicron agglomerates and freeing of polymer, is favored. Only a small number of agglomerates need to degrade to provide a significant increase in the concentration of free poly-

Downloaded At: 11:01 25 January 2011

Copyright © Marcel Dekker, Inc. All rights reserved.

MARCEL DEKKER, INC.
270 Madison Avenue, New York, New York 10016

ORDER REPRINTS

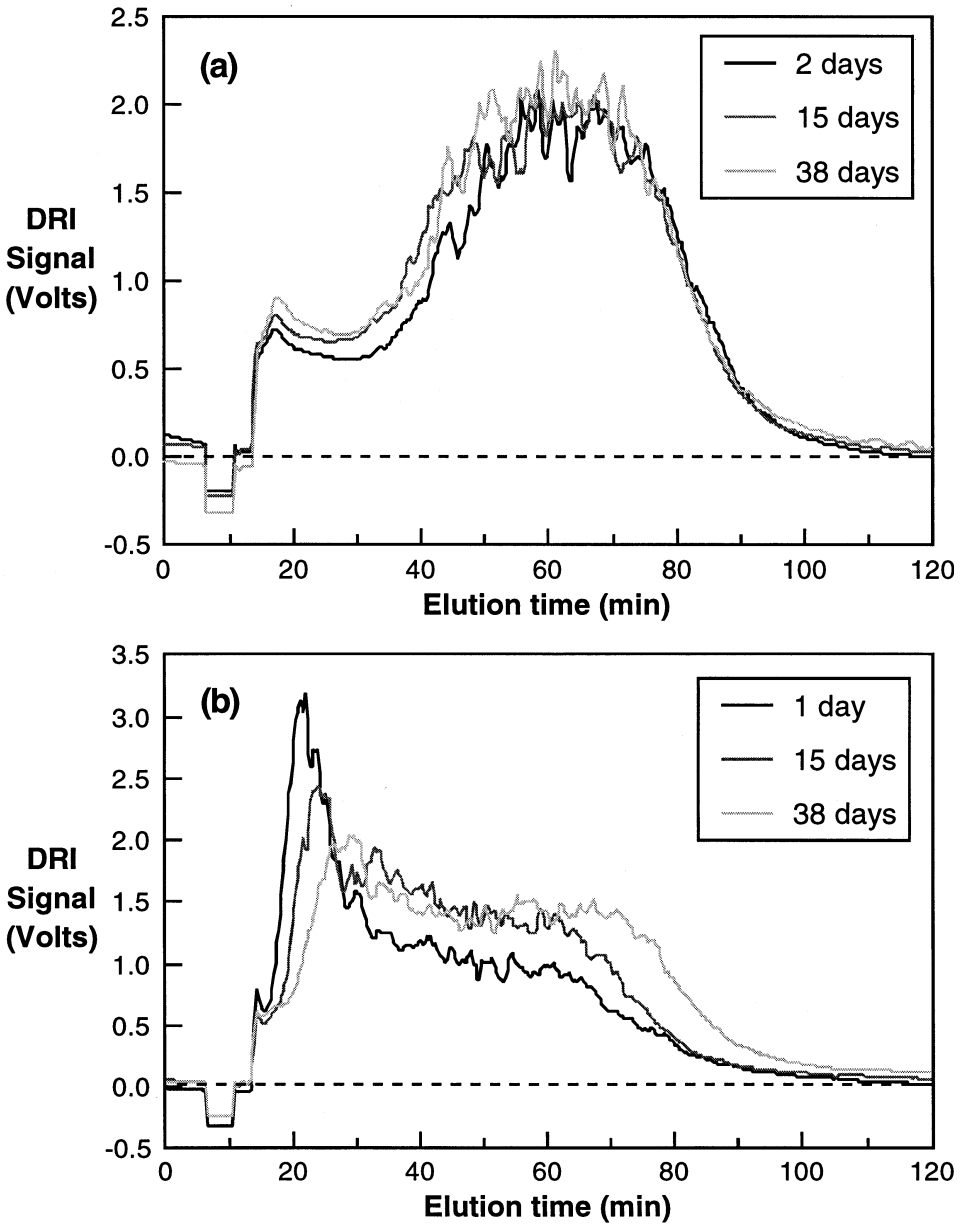

FIG. 5 Fractionation of stock solutions of (a) 4.08 mg·mL^{-1} **A2** and (b) 3.98 mg·mL^{-1} **A1** as a function of solution age.

TABLE 2
Cumulative Elution Concentration Profile, as Percentage of Total DRI Signal, for Commercial Flocculant **A2**

Solution age (days)	Cumulative % mass below M_w			
	$M_w = 3.2 \times 10^6$	1.0×10^7	2.0×10^7	1.0×10^g
2	18.5	48.9	70.7	98.6
15	21.4	53.0	74.5	98.8
38	21.8	53.6	74.6	98.3

Downloaded At: 11:01 25 January 2011

Copyright © Marcel Dekker, Inc. All rights reserved.

MARCEL DEKKER, INC.
270 Madison Avenue, New York, New York 10016

ORDER REPRINTS

mer coils. This result is in agreement with earlier results (21), which reported a decrease in the size of supramicron counts of **A1** with time. Other studies have also postulated that agglomeration may play a role in polyacrylamide solution instability, reflected in viscosity (23–26) and flocculant activity (24, 26) variations over time.

Effects of Concentration on Agglomerates

Agglomeration of PAAm was previously shown to exhibit a definite concentration dependence, with more dilute polymer exhibiting fewer, smaller species (21). Specifically, for the **A1** polymer at concentrations below 1.0 $mg \cdot mL^{-1}$ there was a complete absence of agglomerates. The effect of injecting increasingly dilute **A1** solutions on the agglomeration region (elution times 15–25 minutes) is shown in Fig. 6, in which all signals are scaled to the highest concentration for comparison purposes. Preparing the PAAm solution at 2.07 $mg \cdot mL^{-1}$ causes the agglomerate peak to shift to greater retention, commensurate with smaller agglomerate species eluting under the steric mechanism. The same sample prepared at 0.50 $mg \cdot mL^{-1}$ exhibited a suppression of this region between 15 and 25 minutes, resembling the agglomerate-free **A2** samples. This result qualitatively matched the previously reported concentration effect.

Downloaded At: 11:01 25 January 2011

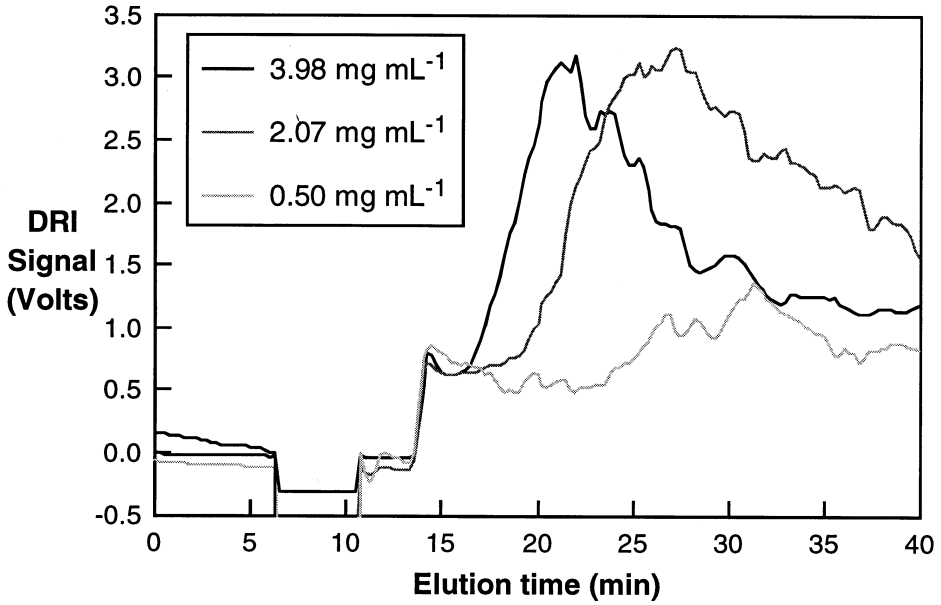

FIG. 6 Effect of **A1** concentration on fractionation. The region displayed shows elution of supramicron species under the steric mode. For comparative purposes, the refractometer responses are linearly scaled to the highest 3.98 $mg \cdot mL^{-1}$ concentration.

Copyright © Marcel Dekker, Inc. All rights reserved.

MARCEL DEKKER, INC.
270 Madison Avenue, New York, New York 10016

ORDER REPRINTS

Dispersion through Added Salt

The substantially higher viscosity of **A1**, relative to the other products as reported in Table 1, is in conflict with the mean molecular masses from light scattering in 0.1 M chloride solutions. Dupuis et al. (27) claimed 0.1 M NaCl is an effective dispersant of PAAm agglomerates, and this has been confirmed with light obscuration measurements (21). Confirmation from flow FFF-MALLS was achieved by injecting PAAm solutions prepared in 0.1 M chloride, as shown in Fig. 7. The large peak is expected because the refractometer is sensitive to the passage of unretained chloride. Upon comparison with chloride-free fractionation (Fig. 7a), **B1** showed little agglomeration, and the presence of chloride resulted in slight changes in the elution profile. For **A1**, agglomerates were obscured somewhat by the DRI sensitivity to the salt, but a distinct shift is observed (Fig. 7b). **A2** gave a viscosity nearly as high as **B1**, yet at only half the mean molecular mass; the elution profile of dispersed **A2** shows a severe change in the molecular mass distribution, with a concentration maximum shifting from 65 to 45 minutes (Fig. 7c). None of the flocculants exhibit anionic character according to ^{13}C NMR, and therefore polyelectrolyte effects upon coil conformation and adsorption are negligible.

For **A2**, the elution profiles from Fig. 7(c) allow an estimate of the amount of material susceptible to dispersion, but quantification requires removal of the unretained "salt peak" emerging at 20 minutes. This region of Fig. 7(c) has been subject to a correction based on the light-scattering signal and the salt-free fractionation. Normalizing the **A2** elution profiles shows that the loss of material eluting in the 60–80 minute period accounts for approximately 15–20% of the total flocculant concentration. This remains a crude estimate due to the assumptions in removing the obscuring salt peak. Dispersion of **A2** therefore effectively increases the free polymer concentration by ca. 15%.

Very different effects were observed for dispersed **A1**. The estimation of the relative change of **A1** agglomeration upon addition of salt, based upon Fig. 7(b), is extremely difficult due to the FFF coelution problem and the salt peak masking the elution profile. However, from Hecker et al. (21), supramicron agglomerates in **A1** were estimated to be 10^{-3}% of the polymer by number, and an order of magnitude less in the presence of chloride. By volume, an agglomerate 10 μm diameter is over 2×10^5 times greater in volume than a single 0.35 μm coil, assuming size-invariant density. Using the simple bimodal population model, a polymer solution consisting of 10^{-3}% 10 μm agglomerates, with the remainder as free coils, would have approximately 18% of the mass of the polymer sample as agglomerates. Although the number concentration of agglomerates is low, their mass and volume contribution has a profound effect.

Downloaded At: 11:01 25 January 2011

Copyright © Marcel Dekker, Inc. All rights reserved.

MARCEL DEKKER, INC.
270 Madison Avenue, New York, New York 10016

ORDER REPRINTS

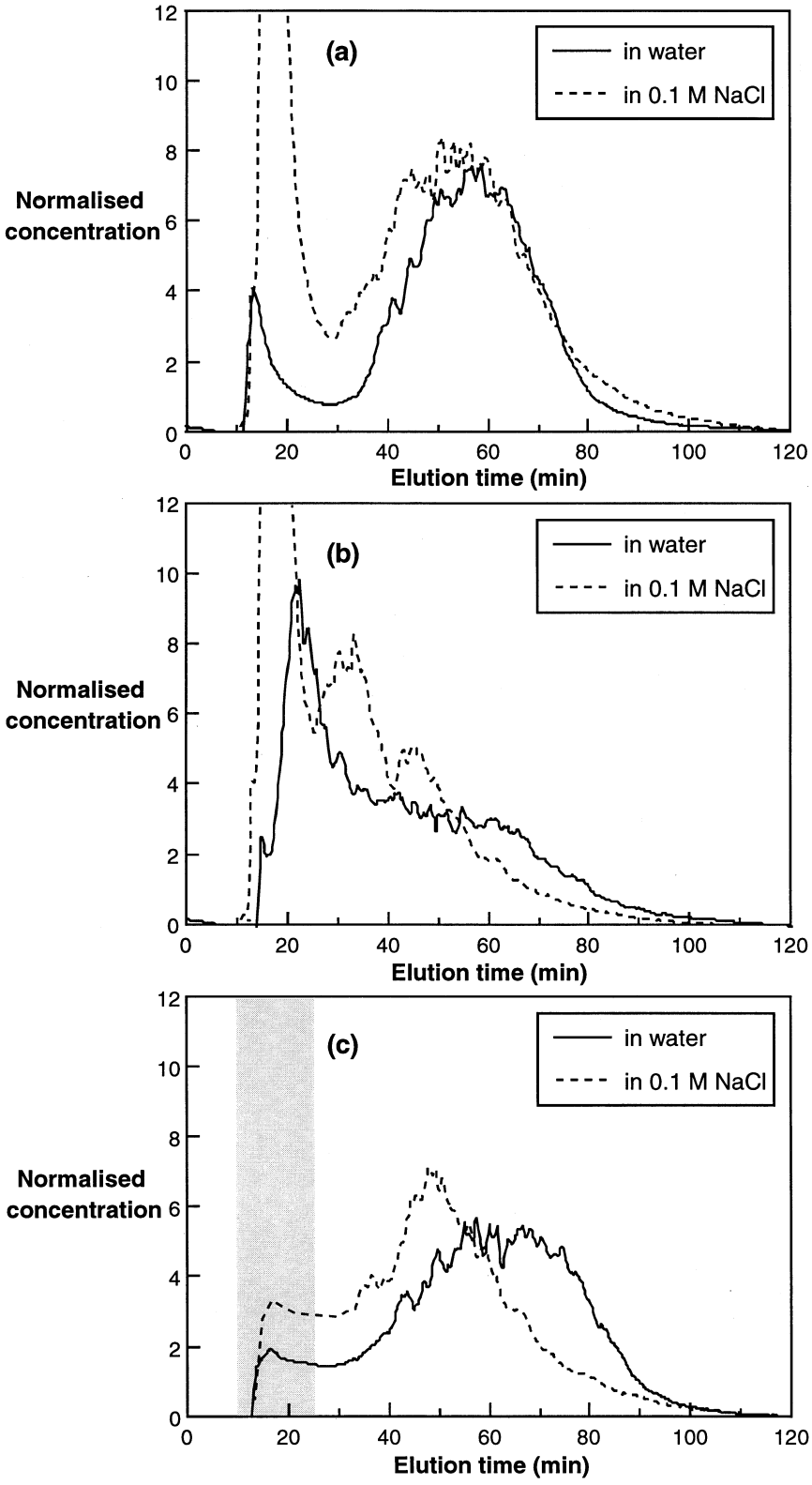

FIG. 7 Effect of preparing polymer stock in 0.1 M NaCl on fractionation for (a) **B1,** (b) **A1,** and (c) **A2.** The large void peak of the salt experiments (dashed line) is attributable to unretained chloride passing the refractometer, and has been subtracted in (c). The refractometer responses are normalized to stock PAAm injections.

Downloaded At: 11:01 25 January 2011

Copyright © Marcel Dekker, Inc. All rights reserved.

MARCEL DEKKER, INC.
270 Madison Avenue, New York, New York 10016

ORDER REPRINTS

Solution State Features

An important remaining issue is to clarify why **B3** and **A2**, with low mean molecular masses, apparently have the widest elution profile of any of the commercial flocculants. Linked to this observation is the tendency of the molecular mass-elution time plot to "flatten" at higher retention, a feature seen in Fig. 2. An explanation is provided if PAAm molecules are considered to exist in one of three solvated states. The first state, occupied by the bulk of the material, is of well-dispersed individual coils. The retention and light scattering of these is well described by theory, and follows the same molecular mass–retention effects of the standards (4). The second state is of supramicron agglomerates, eluting according to the FFF steric mode. The third state is of a few entwined polymers. The FFF separation, sensitive only to diameter, allows their elution after the individual coils, while the MALLS detector observes each molecule in the entwined body as an individual. The mean molecular mass–retention curve then "flattens" as the species radius increases (FFF elution) but the molecular mass remains nearly constant. These different polymer states are shown in Fig. 8, eluting in "zones" from the FFF cell.

Evidence for submicron chain entanglements has also been reported by Ying et al. (28), who detected solution species of about four chains by dynamic light scattering. Preliminary investigations of partially (10%) hydrolyzed polyacrylamides have shown a narrow distribution with full elution before 60 minutes, which may be attributed to charge repulsion discouraging polymer agglomeration effects. The broad elution profiles of the low mean molecular mass commercial flocculants **A2** and **B3** may therefore be due to the presence of these entwined polymers.

The presence of the three "zones" means characterization of PAAm by flow FFF remains viable, but interpretation of the elution profile is not straightforward. Strategies to simplify the elution profiles may be pursued. These include decreasing solution concentration, filtration, modification of flow and field decay rates, or altering the carrier solution.

The concentrations chosen are appropriate for flocculant feed solutions used in mineral processing industries, but since agglomeration and entwinement are concentration-dependent, injection of a more dilute polymer makes elution profile interpretation simpler. However, below a polymer concentration 0.50 $mg \cdot mL^{-1}$ the signal-to-noise ratio for both the MALLS and DRI detectors became an important consideration. It was estimated that at concentrations in the range 0.1 to 0.2 $mg \cdot mL^{-1}$, the data would become intractable. It would therefore not be possible to reduce the amount of sample injected to ensure the presence of discrete polymer chains.

Downloaded At: 11:01 25 January 2011

Copyright © Marcel Dekker, Inc. All rights reserved.

MARCEL DEKKER, INC.
270 Madison Avenue, New York, New York 10016

ORDER REPRINTS

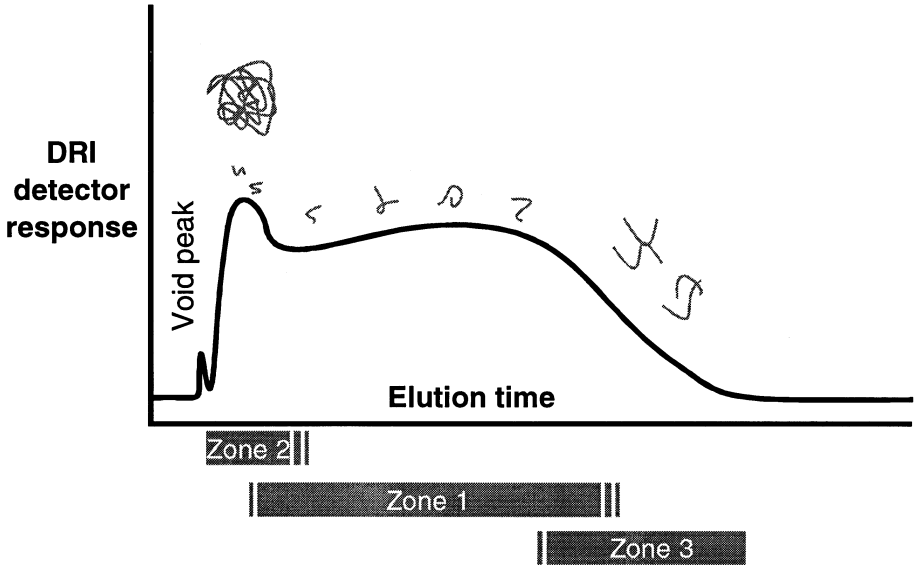

FIG. 8 Generalized elution of the three "phases" of PAAm in aqueous solution. Zone 1 represents well-dispersed PAAm; Zone 2 is agglomerated polymer coeluting with smaller polymers; Zone 3 is submicron diameter "entwined" polymer.

Downloaded At: 11:01 25 January 2011

Filtration through a suitable membrane may be used to remove agglomerates from aqueous PAAm solutions (21). Unfortunately, the solution viscosities at the concentrations used here result in significant backpressure during filtration through membranes with pore sizes of either 0.8 or 3.0 μm. Shear degradation of the polymer becomes a distinct possibility.

Modifications to the flows to shift the position of the FFF mechanism inversion may separate the elution of zone 2 supramicron agglomerates from the submicron species, as the point of steric inversion is empirically known to be dependent on flow conditions, although the relationship is poorly understood even for model latex systems. It may be more promising to apply a delay in the field decay program, which may allow supramicron agglomerates to elute first, separately from the retained submicron material. However, the size distribution is a continuum so a total disengagement of coelution is not possible, while the higher field and longer experiment times may lead to a commensurate loss of resolution.

Adding chloride to the stock solution aided dispersion but affected the refractometer. Matching the carrier solution and polymer stock salinity would allow an elution profile of salt-dispersed polyacrylamide without the salt peak. Unfortunately, the presence of salt is known to decrease the sensitivity of the DRI detector, effectively masking the polymer.

Copyright © Marcel Dekker, Inc. All rights reserved.

MARCEL DEKKER, INC.
270 Madison Avenue, New York, New York 10016

ORDER REPRINTS

CONCLUSIONS

The use of flow field-flow fractionation has been shown to be effective for the separation of commercial polyacrylamides into narrow fractions for characterization by MALLS. Most of the samples studied behaved analogously to polyacrylamide standards. However, some solutions exhibited submicron coil entanglements and supramicron agglomerates. Supramicron agglomerates are difficult to characterize due to the parallel separation mechanisms of FFF. The extent of agglomeration was found to be dependent on the polymer concentration and was also reduced in the presence of dilute sodium chloride.

ACKNOWLEDGMENTS

This research has been supported under the Australian Government's Cooperative Research Centre (CRC) program, through the A. J. Parker CRC for Hydrometallurgy. This support is gratefully acknowledged. R. Hecker is grateful for the support of the ARC by way of an Australian Postgraduate Award through Curtin University of Technology. Elemental analysis was performed by Graeme Rowbottom at the Central Science Laboratory facility at the University of Tasmania.

REFERENCES

1. L. A. Glasgow, *Chem. Eng. Prog.*, *85*(8), 51 (1989).
2. B. M. Moudgil, S. Behl, and T. S. Prakash, *J. Colloid Interface Sci.*, *158*, 511 (1993).
3. R. Hogg, P. Bunnaul, and H. Suharyono, *Min. Metall. Proc.*, *10*, 81 (1993).
4. R. Hecker, P. D. Fawell, A. Jefferson, and J. B. Farrow, *J. Chromatogr. A*, *837*, 139 (1999).
5. J. C. Giddings, *Anal. Chem.*, *67*, 592A (1995).
6. J. C. Giddings, G. C. Lin, and M. N. Myers, *J. Liq. Chromatogr.*, *1*, 1 (1978).
7. Y. S. Gao, K. D. Caldwell, M. N. Myers, and J. C. Giddings, *Macromolecules*, *18*, 1272 (1985).
8. K.-G. Wahlund, H. S. Winegarner, K. D. Caldwell, and J. C. Giddings, *Anal. Chem.*, *58*, 573 (1986).
9. J. J. Kirkland and W. W. Yau, *J. Chromatogr.*, *353*, 95 (1986).
10. J. J. Kirkland, C. H. Dilks, and S. W. Rementer, *Anal. Chem.*, *64*, 1295 (1992).
11. J. J. Kirkland and C. H. Dilks, *Ibid.*, *64*, 2836 (1992).
12. P. J. Wyatt, *Anal. Chim. Acta*, *272*, 1 (1993).
13. M. Martin, *Chromatographia*, *15*, 426 (1982).
14. K. D. Caldwell, in H. G. Barth and J. W. Mays (Eds.), *Modern Methods of Polymer Characterization*, Wiley, New York, NY, 1991, p. 113.
15. J. C. Giddings, *Science*, *260*, 1456 (1993).
16. P. S. Williams and J. C. Giddings, *Anal. Chem.*, *66*, 4215 (1994).
17. S. K. Ratanathanawongs and J. C. Giddings, in T. Provder (Eds.), *Chromatography of Polymers. Characterization by SEC and FFF*, American Chemical Society, Washington DC, 1993, p. 13.

Downloaded At: 11:01 25 January 2011

Copyright © Marcel Dekker, Inc. All rights reserved.

ORDER REPRINTS

18. M. N. Myers and J. C. Giddings, *Anal. Chem.*, *54*, 2284 (1982).
19. K. D. Jensen, S. K. R. Williams, and J. C. Giddings, *J. Chromatogr. A*, *746*, 137 (1996).
20. W.-M. Kulicke, M. Otto, and A. Baar, *Makromol. Chem.*, *194*, 751 (1993).
21. R. Hecker, P. D. Fawell, and A. Jefferson, *J. Appl. Polym. Sci.*, *70*, 2241 (1998).
22. W.-M. Kulicke, R. Kniewske, and J. Klein, *Prog. Polym.*, *8*, 373 (1982).
23. N. Narkis and M. Rebhun, *Polymer* (*London*), *7*, 507 (1966).
24. W. P. Shyluk and F. S. Stow, *J. Appl. Polym. Sci.*, *13*, 1023 (1969).
25. K. L. Gardner, W. R. Murphy, and T. G. Geehan, *Ibid.*, *22*, 881 (1978).
26. M. Chmelir, A. Künschner, and E. Barthell, *Angew. Makromol. Chem.*, *89*, 145 (1980).
27. D. Dupuis, F. Y. Lewandowski, P. Steiert, and C. Wolff, *J. Non-Newtonian Fluid Mech.*, *54*, 11 (1994).
28. Q. Ying, G. Wu, B. Chu, R. Farinato, and L. Jackson, *Macromolecules*, *29*, 4646 (1996).

Received by editor March 23, 1999
Revision received July 1999

Downloaded At: 11:01 25 January 2011

Copyright © Marcel Dekker, Inc. All rights reserved.

MARCEL DEKKER, INC.
270 Madison Avenue, New York, New York 10016

Downloaded At: 11:01 25 January 2011

Request Permission or Order Reprints Instantly!

Interested in copying and sharing this article? In most cases, U.S. Copyright Law requires that you get permission from the article's rightsholder before using copyrighted content.

All information and materials found in this article, including but not limited to text, trademarks, patents, logos, graphics and images (the "Materials"), are the copyrighted works and other forms of intellectual property of Marcel Dekker, Inc., or its licensors. All rights not expressly granted are reserved.

Get permission to lawfully reproduce and distribute the Materials or order reprints quickly and painlessly. Simply click on the "Request Permission/Reprints Here" link below and follow the instructions. Visit the U.S. Copyright Office for information on Fair Use limitations of U.S. copyright law. Please refer to The Association of American Publishers' (AAP) website for guidelines on Fair Use in the Classroom.

The Materials are for your personal use only and cannot be reformatted, reposted, resold or distributed by electronic means or otherwise without permission from Marcel Dekker, Inc. Marcel Dekker, Inc. grants you the limited right to display the Materials only on your personal computer or personal wireless device, and to copy and download single copies of such Materials provided that any copyright, trademark or other notice appearing on such Materials is also retained by, displayed, copied or downloaded as part of the Materials and is not removed or obscured, and provided you do not edit, modify, alter or enhance the Materials. Please refer to our Website User Agreement for more details.

Order now!

Reprints of this article can also be ordered at

http://www.dekker.com/servlet/product/DOI/101081SS100100178